Revision of the NaBO2–H2O phase diagram for optimized yield in the H2 generation through NaBH4 hydrolysis

J. Andrieux, Laetitia Laversenne, Olesia Krol, Rodica Chiriac, Zeinab Bouajila, Richard Tenu, Jean Jacques Counioux, Christelle Goutaudier

Revision of the $NaBO_2$-H_2O phase diagram for optimized yield in the H_2 generation through $NaBH_4$ hydrolysis

Authors : Jérôme ANDRIEUX [a,1 *], Laetitia LAVERSENNE [a,2], Olesia KROL [a], Rodica CHIRIAC [a], Zeinab BOUAJILA [a], Richard TENU [a], Jean Jacques COUNIOUX [a], Christelle GOUTAUDIER [a].

Affiliations :

[a] Université de Lyon, F-69622, Lyon, France ; Université Lyon1, Villeurbanne ; CNRS, UMR 5615, Laboratoire des Multimatériaux et Interfaces.
[1] ID15, European Synchrotron Radiation Facility, Grenoble, France
[2] Institut Néel, CNRS et Université Joseph Fourier, BP 166, F-38042 Grenoble Cedex 9, France

* Corresponding author : European Radiation Synchrotron Facility (ESRF), Beamline ID15, 6 rue Jules Horowitz, 38043 Grenoble Cedex 9, France jerome.andrieux@esrf.fr; Tel. +33 (4) 38 88 19 07; Fax. +33 (4) 76 88 27 07.

Abstract

The binary phase diagram $NaBO_2$-H_2O at ambient pressure, which defines the different phase equilibria that could be formed between borates, end-products of $NaBH_4$ hydrolysis, has been reviewed. Five different solid borates phases have been identified: $NaBO_2 \cdot 4H_2O$ ($Na[B(OH)_4] \cdot 2H_2O$), $NaBO_2 \cdot 2H_2O$ ($Na[B(OH)_4]$), $NaBO_2 \cdot 2/3H_2O$ ($Na_3[B_3O_4(OH)_4]$), $NaBO_2 \cdot 1/3H_2O$ ($Na_3[B_3O_5(OH)_2]$) and $NaBO_2$ ($Na_3[B_3O_6]$), and their thermal stabilities have been studied. The boundaries of the different Liquid+Solid equilibria for the temperature range from -10 to 80 °C have been determined, confirming literature data at low temperature (20 °C ~ 50 °C). Moreover the following eutectic transformation, Liq. → Ice + $NaBO_2 \cdot 4H_2O$, occurring at -7 °C, has been determined by DSC. The Liquid-Vapour domain has been studied by ebullioscopy. The invariant transformation Liq. → Vap. + $NaBO_2 \cdot 2/3H_2O$ has been estimated at 131.6 °C. This knowledge is paramount in the field of hydrogen storage through $NaBH_4$ hydrolysis, in which borate compounds were obtained as hydrolysis reaction products. As a

consequence, the authors propose a comparison with previous $NaBO_2$-H_2O binary phase diagrams and its consequence related to hydrogen storage through $NaBH_4$ hydrolysis.

Keywords: Hydrogen storage, hydrolysis, sodium borohydride, sodium borate, $NaBO_2$-H_2O binary phase diagram, thermodynamics.

1. Introduction

Hydrogen stands today as the highest density energy carrier considered as essential to be developed for a spread use of renewable energy source in alternative to fossil fuel resources. Many researches are focused on H_2 storage system and in particular, chemical compounds for solid state storage. Among the promising compounds, $NaBH_4$, through its hydrolysis (scheme 1 with y = 0) permits an attractive theoretical gravimetric storage density of 10.8 wt.% in safe conditions. Most of the researches related to this system focused on improving the slow kinetics of the scheme 1. In this way, intensive works have demonstrated that noble metal catalysts and cobalt based catalysts were very efficient [1-10]. However, it is paramount to note that beyond the kinetically limitations of the hydrolysis reaction, the main issue to be considered is the practical achievable hydrogen storage capacity [11-12] that can be expressed by the gravimetric hydrogen storage capacity (GHSC). GHSC is defined as the percentage of the gravimetric ratio of recovered hydrogen over the reagents (H_2O and $NaBH_4$) [1]. Actually, experimental hydrolysis reaction never lead to anhydrous metaborate (y = 0) but to hydrated borate compounds as assumed in scheme 1 for $y \neq 0$. The end products have been denoted as $NaBO_2 \cdot yH_2O$ with y, the

[1] $GHSC = \frac{m_{H_2} \cdot 100}{m_{NaBH_4} + m_{H_2O}}$; $m_{H_2O} = f(y)$ according to reaction (1)

pseudo hydration degree [2] [11,12].

As water is a reagent in the hydrolysis, the amount of water needed to complete the reaction increases with the borate pseudo hydration degree (scheme 1). As a consequence, higher the pseudo hydration degree of borate compounds and lower the GHSC (i.e. GHSC = 10.8 wt.% when y = 0; GHSC = 5.5 wt.% when y = 4). This aspect has been pointed out in previous works [11-13] but no study allows predicting which borate compounds can be formed in a precise condition, i.e. what is the highest pseudo hydration degree to be expected and consequently the resulting GHSC.

Borates fundamental knowledge comes from the fact that borates constitute the main form of natural resources of boron. In terms of application, they have been mainly studied for its antiseptic properties and its glass former capabilities. The first thermodynamic investigations of the ternary system H_2O-Na_2O-B_2O_3 has been published by Dukelski [13] in 1906. He pointed out the existence of borates of different compositions at 30 °C. Among all the borate compounds, anhydrous sodium metaborate, $NaBO_2$ [3], has a molecular ratio Na_2O to B_2O_3 of 1:1 [14]. This phase, in presence of water, leads to the formation of hydrated borate compounds ($NaBO_2 \cdot yH_2O$). Two stable borate compounds have been reported at 30 °C in the isothermal section of the system Na_2O-B_2O_3-H_2O [13]: $NaBO_2 \cdot 4H_2O$ [4] and $NaBO_2 \cdot 2H_2O$ [5]. Other isothermal sections of this system have also been determined at 0 °C [15], 45 °C [16], 60 °C [17], 90 °C [18] and 100 °C [19]. For each temperature, we focused our investigation on the isoplethal section $NaBO_2$-H_2O corresponding to the molar ratio Na_2O:B_2O_3 = 1:1.

---

[2] It is to note that this notation does not represent the number of real hydration water molecules as discussed in a recent work [21] and detailed in the included footnotes of the present article.

[3] Structural formula = $Na_3[B_3O_6]$

Table 1 summarizes the reported compounds as a function of the temperature. $NaBO_2 \cdot 4H_2O$ was observed to be stable from 0 °C to 45 °C. $NaBO_2 \cdot 2H_2O$ was characterized in the temperature range 30 ~ 100 °C, but not observed at 0 °C. $NaBO_2 \cdot 1/2H_2O$ was claimed to exist from 45 °C to 100 °C, and $NaBO_2 \cdot 1H_2O$ seems to be stable only for temperatures above 100 °C. However, doubts about the existence and the stability of these two former compounds have been already pointed out [20,21]. Bouaziz [20] has studied in details the binary phase diagram $NaBO_2$-H_2O in the temperature range (30 ~ 300 °C) confirming results obtained by Dukelski [13] about the stability of $NaBO_2 \cdot 4H_2O$ and $NaBO_2 \cdot 2H_2O$. Moreover, two other hydrates were pointed out in this temperature range: $NaBO_2 \cdot H_2O$ and $NaBO_2 \cdot 1/2H_2O$. Even if using similar experimental approaches, Toledano *et al.* [22] have highlighted some differences compared to the work of Bouaziz [20], especially concerning the temperature stability range of $NaBO_2 \cdot H_2O$.

The physical-chemistry knowledge on the different borate compounds was limited to structural characterizations (IR/Raman spectroscopy, TGA and powder X-Ray diffraction): crystallographic investigations have shown that $NaBO_2 \cdot 4H_2O$ nor $NaBO_2 \cdot 2H_2O$ crystallize in the triclinic and monoclinic system respectively [23,24]. No crystallographic structure was determined for $NaBO_2 \cdot 1H_2O$ and $NaBO_2 \cdot 1/2H_2O$ (experimental reference patterns were ICDD #00-014-0678 and #000160242, respectively). Note that another borate compound, $NaBO_2 \cdot 1/3H_2O$ [6], has been characterized in terms of crystallographic structure (space group *Pnma*, a= 8.923 (1), b=7.152 (1), c=9.548 (1) Å) [25]. In addition, we recently reported the synthesis of $NaBO_2 \cdot 2/3H_2O$ [7] [21]. However, these two last compounds were observed neither by thermal decomposition of $NaBO_2 \cdot 4H_2O$ [20,22] nor saturated solution studies [26,27]. All the borate species identified in

---

4 Structural formula = $Na[B(OH)_4] \cdot 2H_2O$

5 Structural formula = $Na[B(OH)_4]$

6 Structural formula = $Na_3[B_3O_5(OH)_2]$

7 Structural formula = $Na_3[B_3O_4(OH)_4]$

the literature have been described as decomposing by non congruent melting and subsequent peritectic reactions which temperatures vary according to the experimental approach used (Table 2).

Very few studies focused on identifying the borate compounds formed after $NaBH_4$ hydrolysis [11,28]. According to Marrero *et al*., $NaBO_2 \cdot 2H_2O$ was identified as the stable borate phase formed after $NaBH_4$ hydrolysis, whatever the reaction conditions were. It is to note that Stepanov *et al.*'s work [28] followed by *ex situ* XRD the borate phase formation after $NaBH_4$ hydrolysis in air at room temperature, i.e. in presence of vapour and CO_2. In this case, the formation of other phases than $NaBO_2 \cdot yH_2O$ ($NaBH_4 \cdot 2H_2O$ and tincalconite ($Na_2B_4O_5(OH)_4 \cdot 3H_2O$) located on the adjacent $Na_2O:B_2O_3 = 1:2$ isoplethic section) can be explained by the presence of CO_2 which modifies the thermodynamic equilibria. The tincalconite formation, resulting from the reaction of borax and carbon dioxide has been highlighted by Krzhizhanovskaya *et al.* [29]. The formation of borax after $NaBH_4$ hydrolysis can be explained from the reaction of sodium borate crystals and solution with dissolved carbon dioxide from the atmosphere [30]. In other words, $NaBH_4$ hydrolysis should be performed under reduced CO_2 atmosphere in order to obtain $NaBO_2 \cdot yH_2O$.

At the sight of the present literature review, the stability of borate compounds, $NaBO_2 \cdot yH_2O$, as a function of temperature need to be clarified, particularly in the low water region of the diagram ($0 < y < 2$). Moreover, previous investigations were focused on studying equilibria in closed reactor for temperature higher than 100 °C, i.e. under non ambient pressure, in order to avoid the vaporization of the borate solution. The lack of information about borate compounds and identification of the borate phases formed after $NaBH_4$ hydrolysis led us to conduct the present study. The authors propose a revision of the binary phase diagram $NaBO_2$-H_2O at ambient pressure, a fundamental knowledge to understand and predict the borate formation through $NaBH_4$ hydrolysis. Identification of every stable borate compounds was

completed by the investigation of binary phases equilibria obtained under ambient pressure in the binary system $NaBO_2$-H_2O. This study highlights the stability of two new borate compounds: $NaBO_2 \cdot 2/3H_2O$ and $NaBO_2 \cdot 1/3H_2O$. Finally, a discussion on the achievable GHSC related to phase equilibria formed in the $NaBO_2$-H_2O system was proposed.

2. Material and methods

As starting materials, commercial $NaBO_2 \cdot 4H_2O$ from ACROS (white powder > 98 %) was used as received. XRD experiment on this reactant, carried out at ambient temperature evidenced the presence of $NaBO_2 \cdot 2H_2O$ (approx. 30 wt.%) in addition to $NaBO_2 \cdot 4H_2O$.

2.1. Borate compounds syntheses

Pure $NaBO_2 \cdot 4H_2O$ was precipitated from a borate solution, $x_{NaBO2} = 0.080$ (x_{NaBO2} is the $NaBO_2$ molar fraction) cooled from 60 °C to room temperature. Large and well faceted crystals in equilibrium with a saturated solution were obtained after ten hours. Lower hydration degree borates, under powder form, were synthesized by solid state dehydration of commercial $NaBO_2 \cdot 4H_2O$ under inert atmosphere (Argon) and atmospheric pressure. Thermal treatments were run with a heating rate of 1 °C.min^{-1} at fixed temperatures of 65 °C, 110 °C, 140 °C, 180 °C and 300 °C ($\Delta T = \pm 1$ °C) for a duration varying from 12 hours to 3 days. In the case of $NaBO_2 \cdot 2/3H_2O$, the synthesis was carried out both by solid state dehydration of commercial $NaBO_2 \cdot 4H_2O$ and $NaBH_4$ hydrolysis as reported previously in [21].

2.2 Borate compounds characterization

Phases were identified by X-Ray powder diffraction using a Panalytical MPD-Pro diffractometer equipped with a X'celerator detector. Bragg-Brentano configuration was used with the Cu $K_{\alpha1+\alpha2}$ radiation ($\lambda_{K\alpha1}$ = 1.5406 Å, $\lambda_{K\alpha2}$ = 1.5444 Å, $\lambda_{K\alpha1}/\lambda_{K\alpha2}$ = 0.5). X-ray diffraction patterns were recorded between 10 and 60 °(2θ) with a step size of 0.016 °(2θ) and an acquisition time of 50 s per step. Polyimide film was covering the sample to prevent from moisture and rehydration. As a consequence, a broad diffusion background was observed at 10-30 °(2θ) with a characteristic peak at ~21 °(2θ). In order to correct the physical displacement of the sample compared to the reference plane, silicon powder (ICDD#00-027-1402) was added to the borate powders. *In situ* X-Ray powder diffraction experiments during thermal treatment were carried out using a Panalytical MPD-Pro diffractometer equipped with a Panton HTK 1200 furnace with similar experimental parameters than RT XRD experiments. In this case an open alumina sample holder (16 mm i.d.) was used. Heat treatments were carried out from ambient temperature to 340 °C, with a heating rate of 2 °C.min^{-1}. Diffraction patterns were collected every 5 °C during heating.

2.3. Borate solutions syntheses and characterization

Borate solutions with controlled composition were prepared by dissolving anhydrous sodium metaborate ($NaBO_2$) in the suitable amount of deionised water.

Boiling temperatures of borate solutions ($0 < x_{NaBO2} < 0.400$, $\Delta x_{NaBO2} = \pm 10^{-3}$) were determined by ebullioscopy using a Cottrell pump in a closed reactor under atmospheric pressure. Boiling temperatures were measured with an alcohol thermometer ($\Delta T = \pm 0.2$ °C). Invariant transformations were studied by Differential Scanning Calorimetry (DSC 821, Mettler-Toledo)

using 40 μL sealed aluminium crucibles. Heating rate was fixed to 0.4 °C.min^{-1} in the temperature range -30 ~ 110 °C. The working atmosphere was maintained at 10^5 Pa Nitrogen.

3. Results

3.1. Identification of borate compounds by XRD

In a preliminary work, we reported on the thermal analysis of commercial $NaBO_2 \cdot 4H_2O$ dehydration, carried out by high resolution variable heating rate TGA [31]. The analysis performed in the temperature range from 25 °C to 340 °C evidenced five successive mass losses. The final product was identified as anhydrous sodium metaborate, $NaBO_2$, by XRD characterization. Table 3 reports the mass losses and the corresponding transformations temperatures observed during the variable heating rate TGA experiment.

In order to get a better understanding of the $NaBO_2 \cdot 4H_2O$ dehydration steps, identification of the stable phases formed upon the dehydration steps was realized by *in situ* XRD starting from commercial $NaBO_2 \cdot 4H_2O$. A first *in situ* XRD experiment (carried out from 25 to 145 °C) pointed out a phase transition at 50 °C assigned to the decomposition of $NaBO_2 \cdot 4H_2O$ into $NaBO_2 \cdot 2H_2O$ (Figure 1). Then, as the temperature increases, $NaBO_2 \cdot 2H_2O$ undergoes a phase transition observed around 100 °C. The transformation leads to a swelling of the sample, responsible for the loss of the diffracted signal and preventing from identifying the compounds formed. In order to overcome the experimental difficulty due to the large sample volume increase around 100 °C, the high temperature range (110 ~ 340 °C) was investigated in a second *in situ* XRD experiment (Figure 2) starting from single phase $NaBO_2 \cdot 2/3H_2O$ obtained by thermal treatment of $NaBO_2 \cdot 4H_2O$ (110 °C during 12 h) [21]. Three phases were evidenced by the *in situ* experiment performed in the temperature range 110 ~ 340 °C. From 150 °C, $NaBO_2 \cdot 1/3H_2O$ was

observed in coexistence with $NaBO_2 \cdot 2/3H_2O$. From 190 °C, $NaBO_2 \cdot 2/3H_2O$, $NaBO_2 \cdot 1/3H_2O$ and $NaBO_2$ were in coexistence. According to the main Bragg peak intensities, the quantity of $NaBO_2 \cdot 2/3H_2O$ and $NaBO_2 \cdot 1/3H_2O$ were inverted in the temperature range 110 ~ 150 °C: thus we suggest that $NaBO_2 \cdot 2/3H_2O$ was decomposed to form $NaBO_2 \cdot 1/3H_2O$. The same behaviour was observed with the relative intensity of Bragg peaks of $NaBO_2 \cdot 1/3H_2O$ and $NaBO_2$ in the temperature range 190 ~ 280 °C. $NaBO_2 \cdot 2/3H_2O$ was no more discernable from 230 °C. Above 280 °C, $NaBO_2$ was the only phase detected.

In order to supplement *in situ* XRD results, different isothermal treatments have been performed starting from commercial $NaBO_2 \cdot 4H_2O$. XRD patterns for compounds heat treated at 65, 110, 140, 180 and 300 °C during 3 days can be found in the Appendix A (Figure A1). XRD pattern for 65 °C evidenced $NaBO_2 \cdot 2H_2O$ (Figure A1.a) whereas $NaBO_2 \cdot 1/3H_2O$ was identified, as single phase, for 110 °C (Figure A1.b), 140 °C (Figure A1.c) and 180 °C (Figure A1.d). Then, $NaBO_2$ was formed for a thermal treatment carried out at 300 °C (Figure A1.e). The temperature stability range of $NaBO_2 \cdot 2H_2O$ and $NaBO_2$ were in accordance both with *in situ* XRD and variable heating rate TGA experiments (Table 3 and [31]). However, isothermal treatments and XRD characterizations evidenced the formation of $NaBO_2 \cdot 1/3H_2O$ from 110 to 180 °C. These results constitute the first experimental characterization of $NaBO_2 \cdot 1/3H_2O$ after heat treatment of $NaBO_2 \cdot 4H_2O$, as this compound was never reported by thermal treatment syntheses [20], TGA analyses [20,22] nor titration [26,27]. Moreover, the formation of $NaBO_2 \cdot 1/3H_2O$ was observed fifty degrees below the formation temperature determined by variable heating rate TGA (162 °C, Table 3).

3.2. Phase equilibria and transformations in the $NaBO_2$-H_2O phase diagram

3.2.1. Liquid+Vapour equilibrium

To our knowledge, no result about a Liquid to Vapour transformation has been reported for the $NaBO_2$-H_2O phase diagram. Previous experiments [20,22] were carried out in closed reactor, i.e. under pressure when temperature exceeds 100 °C. In these experimental conditions, the stability of Liquid+Solid equilibria could have been favoured, the pressure modifying the equilibrium curve Liquid-Vapour.

In the present study, the boundaries of the Liquid+Vapour domain were determined at ambient pressure using ebullioscopy experiments. Figure 3 presents the evolution of the boiling temperature as a function of $NaBO_2$ molar fraction (x_{NaBO2}) defining the boiling point curve. These experimental data are also reported on Figure 4. In the water rich domain, boiling temperature increased from 100.0 °C (pure water) to reach a dwell at 131.6 °C for a borate solution with a $x_{NaBO2} = 0.280$. Above the boiling point curve, the binary phase equilibrium was established between the liquid solution and vapour. In the concentration range $0 < x_{NaBO2} < 0.400$, a temperature dwell was observed at T = 131.6 °C indicating a three phases equilibrium. Vaporization of the liquid phase occurred at T = 131.6 °C in presence of a third phase: the solid phase $NaBO_2 \cdot 2/3H_2O$ (see scheme 2). For temperature higher than 131.6 °C, $NaBO_2 \cdot 2/3H_2O$ was in equilibrium with vapour.

It is to note that the phase transformation occurring at T = 131.6 °C was previously observed by variable heating rate TGA (Step 3, T = 135 °C, Table 3) and wrongly attributed to the dehydration of a hypothetical borate compound ($NaBO_2 \cdot 1{,}2H_2O$) [31]. Results obtained by ebullioscopy measurements clearly demonstrates that the mass loss observed around 135 °C resulted from the vaporization of the liquid formed after the dehydration of $NaBO_2 \cdot 2H_2O$.

3.2.2. Liquid+Solid equilibria

The solubility curve of sodium metaborate (boundary of the Liquid+Solid equilibria) was determined by Nies *et al.* [26] in a temperature range from -10 °C to 120 °C using chemical titration of saturated solutions. These data have been used as published to represent the solubility curve of the binary phase diagram $NaBO_2$-H_2O (Figure 4). For T ~ - 6 °C and x_{NaBO2} ~ 0.040, Nies *et al.* [26] observed a minimum for the solubility curve which corresponds to the eutectic transformation (scheme 3) characterized in the present work by DSC from -30 °C to 30 °C. Different compositions have been studied, i.e. x_{NaBO2} = 0.021, 0.054, 0.095 and 0.161 by DSC experiments and onset temperatures are presented in Table 4. The sharp endothermic peaks define an average temperature of -7 ± 2 °C for scheme 3 (see for example Appendix B, Figure B1.a). According to phase construction rules, a binary phase domain composed of pure ice and $NaBO_2 \cdot 4H_2O$ was defined from -30 °C to -7 °C.

According to Nies' work [26], the solubility's values increased from -6 to 120 °C and two breaks were observed along the solubility curve. The first one, around 50 °C, has been characterized in our work for 0.161 < x_{NaBO2} < 0.265 (Table 4), and corresponds to the peritectic decomposition of $NaBO_2 \cdot 4H_2O$ (scheme 4) as evidenced by *in situ* XRD (Figure 1). The average onset temperature has been measured to 55 ± 2 °C (see for example Figure B1.b in Appendix B), which was in good agreement with literature data (i.e. 53 °C [26]). Thus, a binary phase domain Liquid+$NaBO_2 \cdot 4H_2O$ was defined by these experiments from -7 °C to 55 °C following the phase construction rules. The second break was related to the peritectic decomposition of $NaBO_2 \cdot 2H_2O$ (scheme 5), confirmed by *in situ* XRD (Figure 1). This reaction occurs at 103 ± 2 °C after DSC experiments performed at x_{NaBO2} = 0.333 (Table 4 and Figure B1.c in Appendix B).

Whereas the solubility curve determined by Nies *et al.* [26] at low temperatures and high water content borate solution was in accordance with our experimental data, large discrepancies

were observed at high temperatures between Nies results and our experimental data. For the sake of clarity, experimental results after DSC measurements have been reported on Figure 4. These discrepancies could be partially explained by the tendency to form a metastable state instead of a Liquid+Solid binary phase domain as suggested in recent work [21]. Moreover, the isotherms in Nies *et al.*'s work were obtained, for temperatures above 100 °C, under pressure in order to avoid vaporization of the borate solution. For these reasons, the solubility curve in the temperature range 100.0 ~ 131.6 °C was symbolized in Figure 4 by a dashed line.

3.2.3. Vapour+Solid equilibria

$NaBO_2 \cdot 2/3H_2O$ decomposition temperature has been previously determined by TGA/DSC experiment [21]: peritectic reaction (scheme 6) occurs at 155 ± 2 °C, defining a binary phase domain $NaBO_2 \cdot 1/3H_2O$+Vapour for T > 155 °C. Moreover, variable heating rate TGA experiment (Table 3) indicates a temperature of 250 ± 2 °C for the peritectic decomposition of $NaBO_2 \cdot 1/3H_2O$ according to the scheme 7. As a consequence, a binary phase equilibrium $NaBO_2$+Vapour exists for temperature higher than 250 °C. It is to note that regarding equilibria formed with vapour, this phase was assumed to be a rich water phase, almost pure vapour for temperatures higher than 100 °C, as borate compounds' saturation vapour pressure was supposed to be high. As no experimental data was available to highlight this point, vapour domain was represented by a dashed line on Figure 4.

4. Discussion

4.1. Borate compounds formation and stability

Five borate compounds have been identified in the $NaBO_2$-H_2O system: $NaBO_2 \cdot 4H_2O$, $NaBO_2 \cdot 2H_2O$, $NaBO_2 \cdot 2/3H_2O$, $NaBO_2 \cdot 1/3H_2O$ and $NaBO_2$. These compounds were stable at

room temperature (characterized at room temperature by XRD after heat treatment synthesis). Hydrated borates ($NaBO_2 \cdot 4H_2O$, $NaBO_2 \cdot 2H_2O$, $NaBO_2 \cdot 2/3H_2O$, $NaBO_2 \cdot 1/3H_2O$) decomposed by peritectic transformations according to schemes 4 to 7 respectively.

The present results i) refine literature knowledge about $NaBO_2 \cdot 4H_2O$ and $NaBO_2 \cdot 2H_2O$, ii) highlight the existence and specify the stability domain of $NaBO_2 \cdot 2/3H_2O$, $NaBO_2 \cdot 1/3H_2O$ and $NaBO_2$ (the two first compounds were observed neither by thermal decomposition of $NaBO_2 \cdot 4H_2O$ [20,22] nor saturated solution studies [26,27]), iii) state on the non existence of $NaBO_2 \cdot 1H_2O$ and $NaBO_2 \cdot 1/2H_2O$ as stable compounds.

Concerning this last point, previous works reporting on the observation of the $NaBO_2 \cdot 1H_2O$ and $NaBO_2 \cdot 1/2H_2O$ compounds were related to non atmospheric pressure studies [20,22,26] and even if referring to similar experimental conditions, discrepancies were observed, in particular in the Toledano *et al.*'s [22] and Bouaziz's [20] works where $NaBO_2 \cdot 1/2H_2O$ stability was discussed. It is also to note that the only crystallographic data available for these compounds [20] were experimental powder XRD patterns as no single crystal characterization of these compounds as well as no single phase synthesis were carried out to our knowledge. The experimental powder XRD patterns were not sufficient enough to provide a clear identification of the compounds. Thus, from the non observation of $NaBO_2 \cdot 1H_2O$ and $NaBO_2 \cdot 1/2H_2O$ after characterization techniques as TGA, DSC and X-ray Diffraction, the authors state on the non existence of these compounds as stable phase in the binary phase diagram $NaBO_2$-H_2O at atmospheric pressure, i.e. in similar conditions compared to that corresponding to the borate formation through $NaBH_4$ hydrolysis.

The temperatures of formation of $NaBO_2 \cdot 1/3H_2O$, determined by high resolution variable heating rate TGA (T = 162 °C) and *in situ* XRD (T = 110 °C), show a fifty degrees gap. The difference in observed temperatures can be attributed to the role of the water partial pressure in

the borate compound formation. Actually, the main configuration difference between the two experiments was the size of the surface exchange between the sample and its gaseous atmosphere: variable heating rate TGA experiment was carried out in a predrilled cap closed crucible, characterized by a low surface exchange (0.35 mm^2), whereas *in situ* XRD characterisations were carried out using a open alumina sample holder with a 201 mm^2 surface exchange. The low surface exchange favours a water partial pressure value close to that of equilibrium conditions. In this work, the dehydration temperature of each compound have been defined using thermal analysis experiments (TGA and DSC), these techniques minimizing the effect of the water partial pressure. To our knowledge, no detailed study on borate compounds' partial pressure has been reported. The present work highlights a decrease of 50 °C for the decomposition temperature of $NaBO_2 \cdot 1/3H_2O$. Actually, thermal treatment carried out at 110 °C during 12 h led to the formation of $NaBO_2 \cdot 2/3H_2O$ [21] whereas longer treatment (3 days) led to the formation of $NaBO_2 \cdot 1/3H_2O$. Compared to the conventional borate compound formation, i.e. invariant transformation for a given temperature, this work evidences another way for borate compounds formation in which the compound decomposition was due to a decrease of the vapour pressure. Thus, the determination of the vapour pressure related to each borate compound should lead to a better understanding of the dehydration mechanism.

The evidence of $NaBO_2 \cdot 2/3H_2O$ and $NaBO_2 \cdot 1/3H_2O$ formation under atmospheric pressure constitutes not only a fundamental difference compared to previous literature studies but a key point for hydrogen storage through $NaBH_4$ hydrolysis: the formation of these low hydration degree borates, compared to $NaBO_2 \cdot 2H_2O$ commonly observed [11], constitutes a way of a potential significant increase of the GHSC. Moreover, the present results suggest that the vapour pressure is a significant parameter for the monitoring of the temperature formation of these compounds: as an example, $NaBO_2 \cdot 1/3H_2O$ can be formed at lower temperature by decreasing

the vapour pressure over the compound.

4.2. $NaBO_2$-H_2O phase diagram

A compilation of all the results is proposed under the form of the binary phase diagram plotted in Figure 4 in the temperature range -30 ~ 300 °C.

This complete revision of the $NaBO_2$-H_2O binary phase diagram points out main differences compared to the previous ones [20,22] in particular in the rich water part ($x_{NaBO2} < 0.333$) and in the low water part ($x_{NaBO2} > 0.333$) of the binary phase diagram.

First, in the rich water part of the diagram ($x_{NaBO2} < 0.333$), Liquid+Vapour biphasic domain has been described as a function of the $NaBO_2$ molar fraction in the temperature range 100 ~ 131.6 °C. In this domain, vapour was in equilibrium with a borate saturated solution. At 131.6 °C, the scheme 2 occurred and above 131.6 °C, solid borate compounds were in equilibrium with vapour.

Second, concerning the low water part of the binary phase diagram ($x_{NaBO2} > 0.333$), the existence of two borate compounds has been pointed out: $NaBO_2 \cdot 2/3H_2O$ ($x_{NaBO2} = 0.666$) and $NaBO_2 \cdot 1/3H_2O$ ($x_{NaBO2} = 0.750$). These compounds were stable until 155 °C and 250 °C respectively and were involved in different phase equilibria.

The synthesis of $NaBO_2 \cdot 2/3H_2O$ single crystals [21] can be achieved in the binary phase domain Liquid+$NaBO_2 \cdot 2/3H_2O$ from 103 to 131.6 °C. However, most of the attempts to synthesize the crystallized compound in equilibria with its saturated borate solution felt down in the formation of a metastable gel state. It is to note that for a temperature lower than 103 °C, $[B(OH)_4]^-$ ions were present in the solution (see for example the works of Anderson *et al.* for T = 30 °C [32] and Edwards *et al.* [33]). Thus, $NaBO_2 \cdot 4H_2O$ ($Na[B(OH)_4] \cdot 2H_2O$) and $NaBO_2 \cdot 2H_2O$ ($Na[B(OH)_4]$) were observed as the stable phases in equilibrium with saturated borate solution in this temperature range (Figure 4). To our knowledge, there was no available data about the nature of

the polyanions in the saturated borate solution for temperature higher than 103 °C. We suggest that the nature of the main polyanion in presence might be close to $[B_3O_4(OH)_4]^{3-}$, this polyanion being the fundamental building block (FBB) of $NaBO_2 \cdot 2/3H_2O$ [21]. This polyanion could favour the polymerisation between chains or sheets leading to a gel formation. Indeed $[B_3O_4(OH)_4]^{3-}$ is based on a B-O cycle, with a maximum out of the plane deviation of O5 of 0.35 Å [21], giving the possibility to form chains and sheets. Second this polyanion contains both hydroxyl groups and bivalent oxygen atoms leading to the possibility of hydrogen bonding formation. A similar behaviour has been observed and explained for other borate system, like metaboric acid HBO_2(II), where strong hydrogen bonds lead to endless zigzag chains of composition $B_3O_4(OH)(OH_2)$ directed along one axis with H_2 bonds forming links between the chains of different layers as well as between chains of the same layer [30]. To sum up, the nature of the stable polyanion as a function of the temperature could cause differences in the B-O network of the saturated solution: i) for T < 100 °C, the presence of $[B(OH)_4]^-$ would favour the crystallisation of $NaBO_2 \cdot 4H_2O$ and $NaBO_2 \cdot 2H_2O$, ii) for T > 100 °C, presence of $[B_3O_4(OH)_4]^{3-}$ could lead to the polymerisation of the saturated solution resulting in a metastable viscous gel. Further work is required to evidence the presence of $[B_3O_4(OH)_4]^{3-}$ ions in borate solutions at high temperature (T > 100 °C) since the formation of metastable gel is a significant technical issue for the implementation of $NaBH_4$ hydrolysis. Understanding the way the gel state was formed would be very helpful in the search for destabilizing this metastable state since it constitutes a key point for future industrial applications.

As a consequence of this metastable state evidence, we have considered, in the review of the binary phase diagram, a biphasic domain Liquid+$NaBO_2 \cdot 2/3H_2O$ from 105 °C to 131.6 °C but the solubility curve of this domain has been plotted in dashed line, as investigations are still in progress to define this part of the solubility curve (Figure 4).

Beyond the fundamental interest of determining the $NaBO_2$-H_2O phase diagram in the temperature range -30 ~ 300 °C, the present work constitutes an invaluable tool for optimisation of the hydrogen capacity of $NaBH_4$ hydrolysis. Actually the GHSC of $NaBH_4$ hydrolysis is related to the reaction stoichiometry (ratio $NaBH_4/H_2O$) but the $NaBH_4/H_2O$ ratio can be optimized as a function of the nature of the borate compounds formed. Depending on the temperature and composition, that means depending on the thermodynamic equilibrium described in the $NaBO_2$-H_2O phase diagram, the ratio of "hydriding" water (trapped in the hydrated borate) over "reacting" water (involved in the hydrolysis) can vary. If x_{NaBO2} represents the $NaBO_2$ molar fraction and y the pseudo hydration degree of borate compounds, the empirical relation between x_{NaBO2} and y, i.e. the relation between the binary phase diagram $NaBO_2$-H_2O and the $NaBH_4$ hydrolysis, is given by scheme 8.

In the present work, the phase domains of the diagram were investigated using either borate solutions prepared both from dissolution of anhydrous $NaBO_2$ and from reaction product of $NaBH_4$ hydrolysis in order to be as close as possible to the $NaBH_4$ hydrolysis conditions.

In the next, we discuss the specific consequence deduced from the revised $NaBO_2$-H_2O phase diagram, supported on the following assumptions regarding the $NaBH_4$ hydrolysis reaction:

- A complete reaction was assumed, leading to the formation of the stable compounds evidenced in the $NaBO_2$-H_2O diagram.
- GHSC calculation was only based on the hydrolysis reaction (scheme 1) and does not take into account the overall system required to perform $NaBH_4$ hydrolysis.

Table 5 presents the theoretical GHSC expected after formation of the borate compounds

evidenced in the present work. Note that in the hypothesis that the final hydrolysis product is a single phase liquid borate solution, the GHSC cannot be higher than 2.56 wt.% at 25 °C [34] with an initial $NaBH_4$ solution that contains 12.4 g $NaBH_4$ per 100 g H_2O. This limitation results from the fact that the GHSC was limited by the borate anion solubility (21.6 g $NaBO_2$ per 100 g H_2O at 25 °C [26]) and not by the BH_4^- solubility (35.6 g $NaBH_4$ per 100 g H_2O at 24 °C, [35]). The authors pointed out that even though the "all liquid" reaction (reactant and final products are purely liquid at 25 °C) appears technologically attractive, the resulting GHSC is very weak and, as suggested in other works [11,12], worthwhile GHSC can only be achieved with solid borate compound as final products. The highest GHSC of $NaBH_4$ hydrolysis, i.e. 10.8 wt.%, is only achievable by direct formation of anhydrous $NaBO_2$ and H_2, following the so called "ideal" hydrolysis, i.e. following the reactant ratio $NaBH_4$:H_2O = 1:2 [36-39]. The conditions to form $NaBO_2$, deduced from the binary phase diagram, is at high temperature (T > 250 °C) where $NaBO_2$ coexists with Vapour. Highest GHSC would be observed when the vapour formed would be recovered to hydrolyse unreacted $NaBH_4$. $NaBO_2$ also appears, at lower temperature (-30 ~ 250 °C), in the Solid + Solid binary phase domain ($NaBO_2 \cdot 1/3H_2O$ + $NaBO_2$). In this case, the presence of $NaBO_2 \cdot 1/3H_2O$ can lead to a decrease of the GHSC (10.0 wt.%). Moreover, the achieving of pure $NaBO_2$ implies the overcoming of strong difficulties as, for example, a high temperature reaction or a weak diffusion coefficient in solid state. As a consequence the so called "ideal" hydrolysis reaction, i.e. $NaBH_4$:H_2O = 1:2 could not be envisaged for a real industrial application.

According to the present work, worth GHSC in the order of 9-10 wt.% can be reached for operating temperature not higher than 132 °C, the final borate compounds being $NaBO_2 \cdot 2/3H_2O$ or $NaBO_2 \cdot 1/3H_2O$. Two ways are proposed to reach such high GHSC: 1) direct synthesis of the

less hydrated compound (described hereafter) or 2) carrying out a 1:6 hydrolysis reaction in order to obtain $NaBO_2 \cdot 4H_2O$ and then the latter compound is dehydrated to the desired final product, the recovered water becoming available for subsequent hydrolysis. Both ways have their own advantages and drawbacks, the second one requiring for example a two steps process to achieve the theoretical GHSC.

Concerning the direct synthesis of the less hydrated compound, we consider, for the discussion, the synthesis of $NaBO_2 \cdot 2H_2O$ for a 1:4 hydrolysis reaction stoichiometry and a temperature of 70 °C. It is not clear if the reaction first leads to $NaBO_2 \cdot 4H_2O$ which dehydrates to form the desired product or if the final product is directly formed during the reaction. In other words, what is the chemical pathway leading to $NaBO_2 \cdot yH_2O$ from $NaBH_4$ hydrolysis? To our knowledge, there was only one study detailing this point [11]. In the Marrero-Alfonso's work [11], reactions were carried out at T = 100 °C by reacting $NaBH_4$ and vapour inside a closed reactor. The final product after reaction was $NaBO_2 \cdot 2H_2O$ under a variety of reaction conditions. Marrero-Alfonso *et al.* conclude that $NaBO_2 \cdot 2H_2O$ will be the stable form at temperature up to 105 °C, and that the degree of hydration of the product does not appear to be a direct function of the water/hydride ratio of the hydrolysis [11]. The present work agrees with the latter remark but the temperature has also to be taken into account to predict the nature of the phase formed by $NaBH_4$ hydrolysis. $NaBO_2 \cdot 2H_2O$ will not be the stable phase if reaction is carried out at ambient temperature for example, but $NaBO_2 \cdot 4H_2O$. Thus Marrero-Alfonso *et al.* mentioned that $NaBO_2 \cdot 2H_2O$ remained stable even if reaction temperature was slightly in excess of 105 °C whereas our work indicates a peritectic decomposition at 103 °C (scheme 5). The non observation of $NaBO_2 \cdot 2/3H_2O$ by Marrero-Alfonso *et al.* for temperature higher than 103 °C could be explained either because the reaction was carried out in a closed reactor, i.e. under pressure, modifying the thermodynamic equilibria or because of the slow dehydration kinetics of $NaBO_2 \cdot 2H_2O$. The third hypothesis is

$NaBO_2 \cdot 2H_2O$ could be decomposed *in situ* into a Liquid+Solid following for example the scheme 5. In this case $NaBO_2 \cdot 2/3H_2O$ could be formed *in situ*. However, the reaction being carried out in a closed reactor, the overall composition remains constant and from the Liquid+Solid equilibria, $NaBO_2 \cdot 2H_2O$ will be reformed upon cooling. In addition, even for experiments carried out at ambient temperature, one should keep in mind that hydrolysis reaction is exothermic [40] and locally the temperature might be higher than the dehydration temperature of $NaBO_2 \cdot 4H_2O$, especially if the reactor is thermally insulated.

One other fundamental remark concerns the feasibility of the formation of low pseudo hydration degree borate compound through $NaBH_4$ hydrolysis. According to Figure 4, each compound even the less hydrated one could be formed at ambient temperature. However, regarding the way to perform $NaBH_4$ hydrolysis, reaction of liquid water and solid $NaBH_4$ ends up most of the time to local heterogeneities of the reaction stoichiometry [5,41-43]. For a given temperature, the most hydrated stable borate should be first formed, leading to a non equilibrium state with the sequence $H_2O/NaBO_2 \cdot yH_2O/NaBH_4$. Thus, from a microstructure point of view, reaction of water with $NaBH_4$ grain might lead to the formation of a borate layer at the surface of the $NaBH_4$ grain. As a consequence, borate compound formation could act as a strong diffusion barrier for water. The conversion of $NaBH_4$ will end up into very slow kinetics as chemical reaction between two solids ($NaBH_4$ and $NaBO_2 \cdot yH_2O$) falls into very weak diffusion coefficients leading to incomplete $NaBH_4$ hydrolysis and as a consequence to a drop of the effective GHSC.

A first approach to overcome this limitation could be to increase the surface/volume ratio, i.e. to decrease the size of the $NaBH_4$ grain. Recent investigations were focused on synthesizing nanosized chemical hydrides in order to modify thermodynamics of the hydride decomposition in temperature [44,45]. The authors propose to perform $NaBH_4$ hydrolysis based on nanosized

$NaBH_4$ powder. The consequence could be an increase of the GHSC as $NaBH_4$ is mostly consumed but also an increase of the kinetics related to an increase of the specific surface where $NaBH_4$ hydrolysis could take place. It could be promising to combine this approach with the use of vapour instead of liquid water in order also to avoid local heterogeneity. There is to our knowledge no study combining these two approaches.

A second approach is based on the knowledge of the binary phase diagram $NaBO_2$-H_2O. As limitations come from a separation of reactants by a borate layer and weak solid state diffusion between two solids, the hydrolysis should be restricted to conditions leading to a Liquid+Solid binary phase domain. The aim is to entirely dissolve $NaBH_4$ to lead to an equilibrium between a saturated borate solution and $NaBO_2 \cdot yH_2O$ crystals. Three different Liquid+Solid domains are identified from Figure 4. Liquid+$NaBO_2 \cdot 4H_2O$ for a $NaBO_2$ molar fraction from 0.040 to 0.200 and a temperature range from -7 °C to 55 °C. This domain corresponds to hydrolysis performed with a ratio $NaBH_4$:H_2O from 1:26 to 1:6 (according to scheme 1 and scheme 8) and lead to the formation of $NaBO_2 \cdot 4H_2O$ with an associated GHSC of 5.5 wt.% (Table 5). Increasing the temperature, from 55 to 103 °C, a new Liquid+Solid domain was formed: Liquid+$NaBO_2 \cdot 2H_2O$. A $NaBO_2$ molar fraction from 0.138 to 0.333 corresponds to a reaction stoichiometry of 1:8.25 to 1:4 (ratio $NaBH_4$:H_2O). In this domain, a maximum GHSC of 7.3 wt.% was related to the $NaBO_2 \cdot 2H_2O$ formation. The last Liquid+Solid domain was observed in Figure 4 for a temperature range 105 ~ 131.6 °C and a $NaBO_2$ molar ratio (reaction stoichiometry) from 0.258 (1:4.87) to 0.600 (1:2.66). In these conditions, Liquid+$NaBO_2 \cdot 2/3H_2O$ equilibrium could be formed and the maximum GHSC related to this domain is 9.3 wt.%. In all of these three Liquid+Solid phase domains, the GHSC will be as high as the liquid proportion will be weak. Figure 5 sums up the results concerning the hydrolysis stoichiometry, temperature and expected GSHC according to the above discussion.

To conclude, the three Liquid+Solid binary phase domains (Figure 4) define the reaction conditions to achieve high GHSC through $NaBH_4$ hydrolysis. The Liquid+$NaBO_2 \cdot 2/3H_2O$ binary phase equilibrium (100 °C < T < 131.6 °C) with, for example, a $NaBO_2$ molar fraction of 0.6 (i.e. $NaBH_4$:H_2O = 1:2.66), represents, the highest GHSC that could be expected from $NaBH_4$ hydrolysis (around 9.3 wt.%) from a Liquid+Solid phase equilibria. Further work is required to make clear the real conditions but the $NaBO_2$-H_2O binary phase diagram should stand as a reference to predict phases formation through $NaBH_4$ hydrolysis.

5. Conclusion

A revision of the $NaBO_2$-H_2O binary phase diagram is proposed in this work. Taking into account that experiments have been carried out under ambient pressure, this diagram stands as a fundamental knowledge in the $NaBH_4$ hydrolysis. The main result concerns the low water region of the diagram, where two new borate compounds have been identified: $NaBO_2 \cdot 2/3H_2O$ and $NaBO_2 \cdot 1/3H_2O$. According to their low hydration degree, these compounds seem to be interesting in the $NaBH_4$ hydrolysis because GHSC could be expected around 10.0 wt.%. Moreover, this work proposes a first approach in the way to use this thermodynamic knowledge to tune the $NaBH_4$ hydrolysis conditions (temperature and stoichiometry) in order to improve GHSC. Different binary phase equilibria have been defined according to the binary phase diagram, especially the Liquid+Solid domains which determine the hydrolysis conditions to perform complete reactions and achieve highest GHSC through $NaBH_4$ hydrolysis.

Acknowledgements

The authors acknowledge the region “Rhône-Alpes” for the PhD thesis fellowship (Cluster 7 ENERGIE) and the French National Research Agency (ANR, PAN-H program) for financial support.

Figure captions

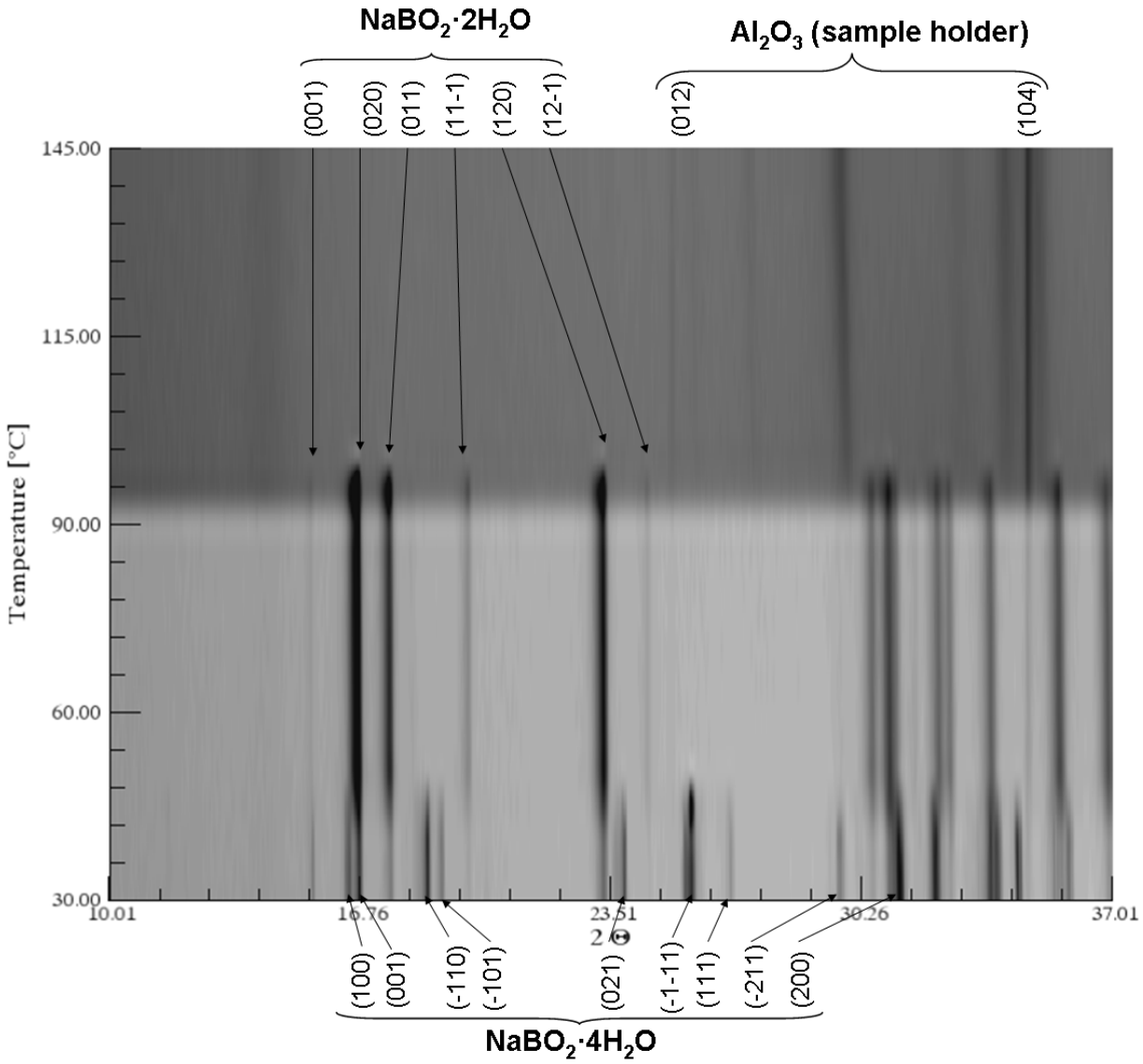

Figure 1. XRD patterns as a function of the temperature (25-115 °C, 2 °C.min^{-1}). Starting material is commercial $NaBO_2 \cdot 4H_2O$. Darker the peak, higher the intensity. Peaks identification was performed by comparison with ICDD reference pattern #01-076-0755 for $NaBO_2 \cdot 4H_2O$ and #01-081-1512 for $NaBO_2 \cdot 2H_2O$.

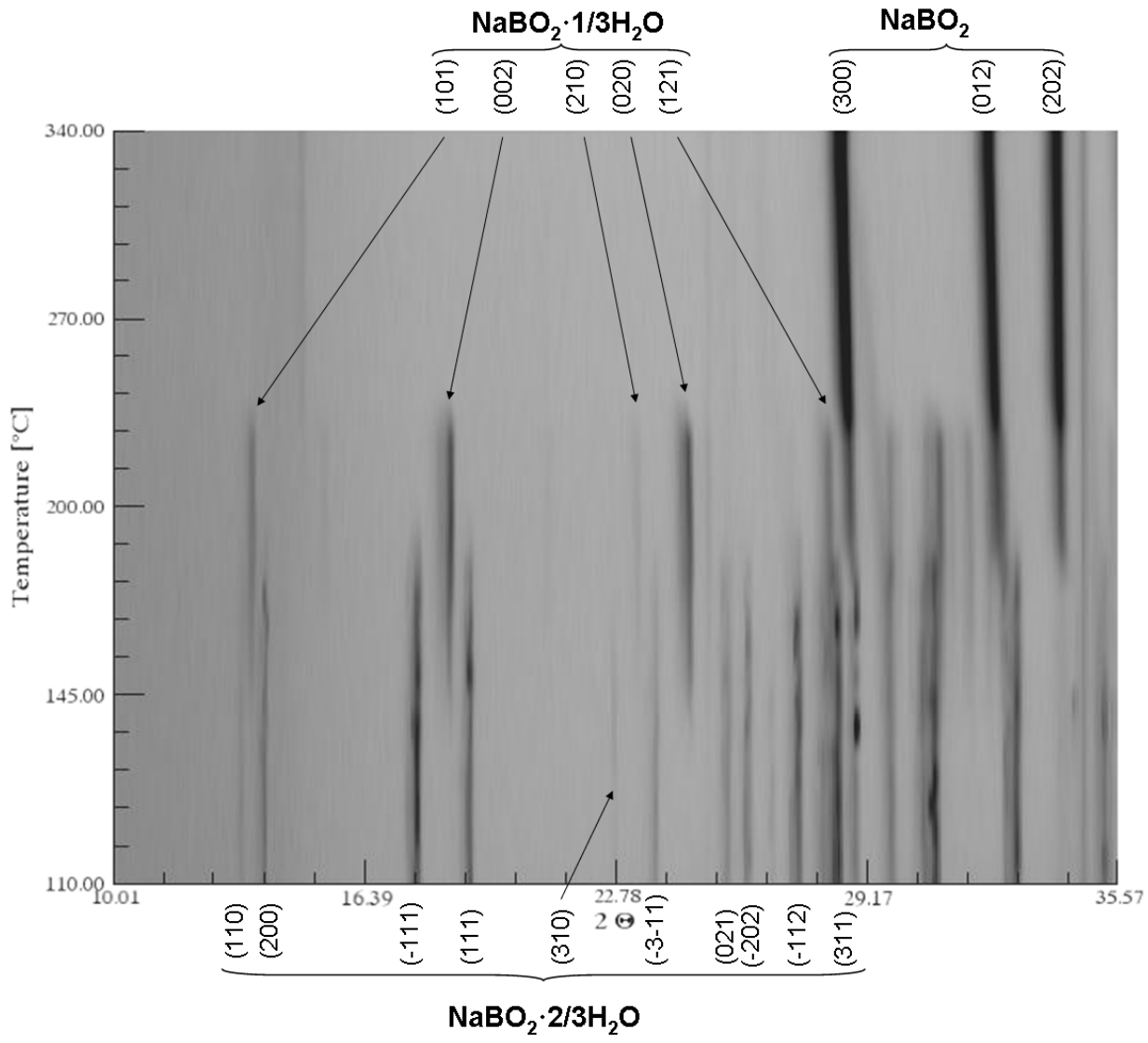

Figure 2. XRD patterns as a function of the temperature (110-340 °C, 2 °C.min^{-1}). Starting material is $NaBO_2 \cdot 2/3H_2O$. Darker the peak, higher the intensity. Peaks identification was performed by comparison with ICDD reference pattern #00-035-0440 for $NaBO_2 \cdot 1/3H_2O$ and #00-032-1046 for $NaBO_2$. Peaks identification of $NaBO_2 \cdot 2/3H_2O$ refers to the work of Andrieux et al. [21].

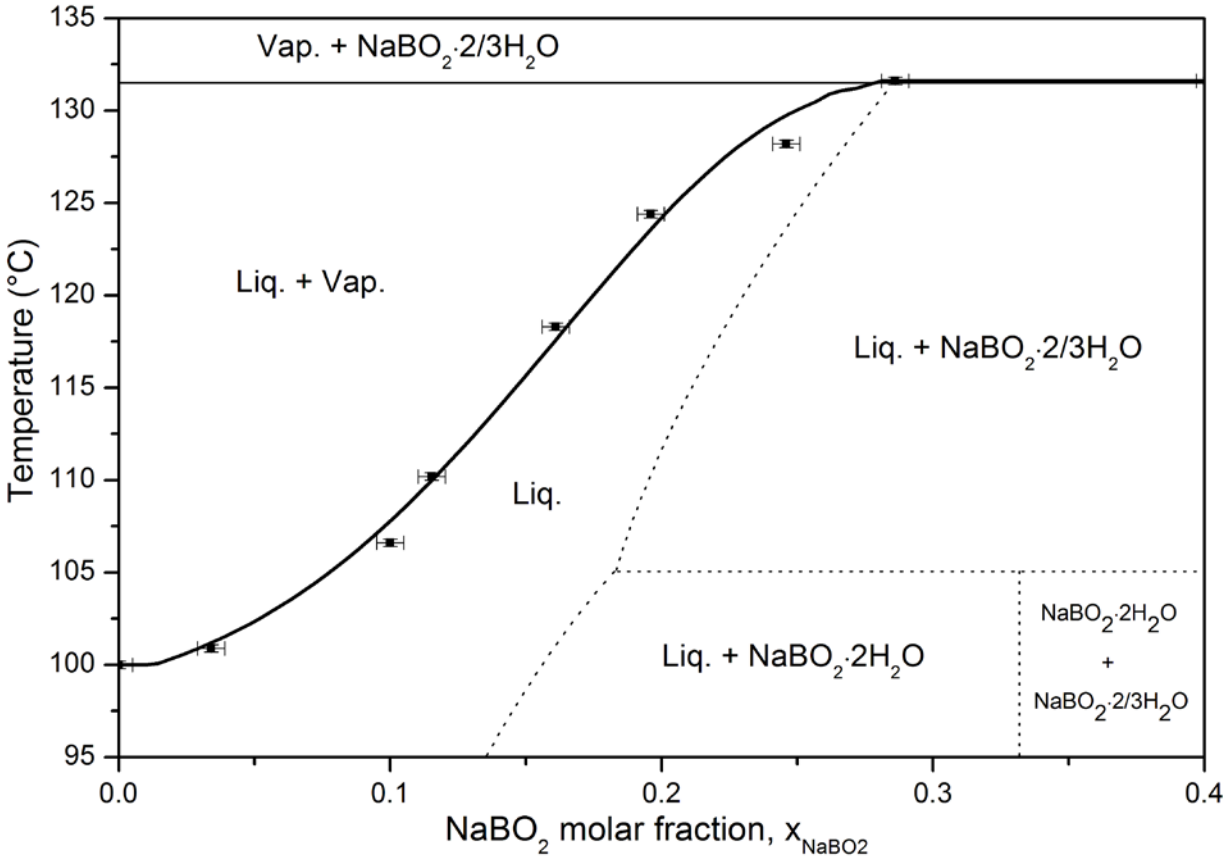

Figure 3. Evolution of the Liquid+Vapour equilibrium temperature as a function of the $NaBO_2$ molar fraction, x_{NaBO2}. Schematic dashed line solubility curve and invariant transformation ($NaBO_2 \cdot 2/3H_2O$+Liq.→$NaBO_2 \cdot 2H_2O$) were reported to facilitate the visualisation of the different equilibria.

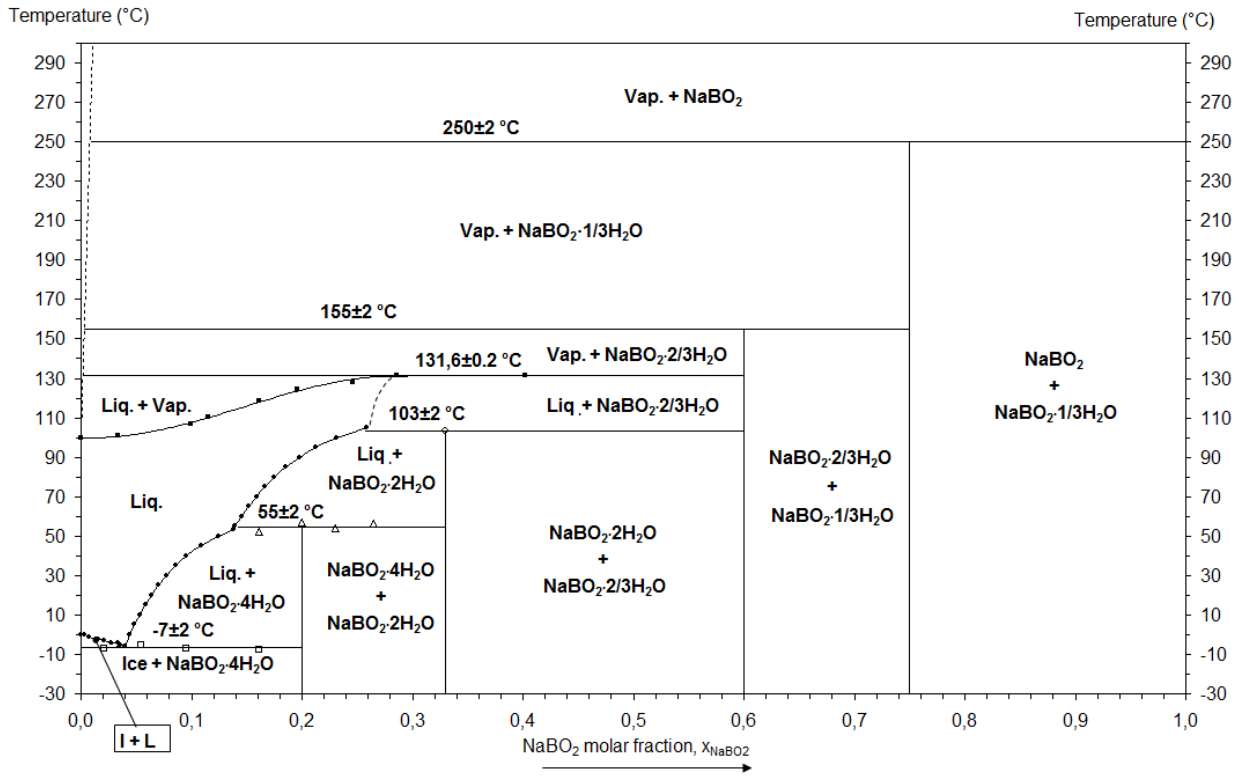

Figure 4. Revised binary phase diagram of the system $NaBO_2$-H_2O. (●) Solubility curve after Nies et al. work [26]. (■) Liquid+Vapour equilibrium temperatures after ebullioscopy

experiments. Onset temperatures after DSC experiments for scheme 3 (□), scheme 4 (Δ) and scheme 5 (○).

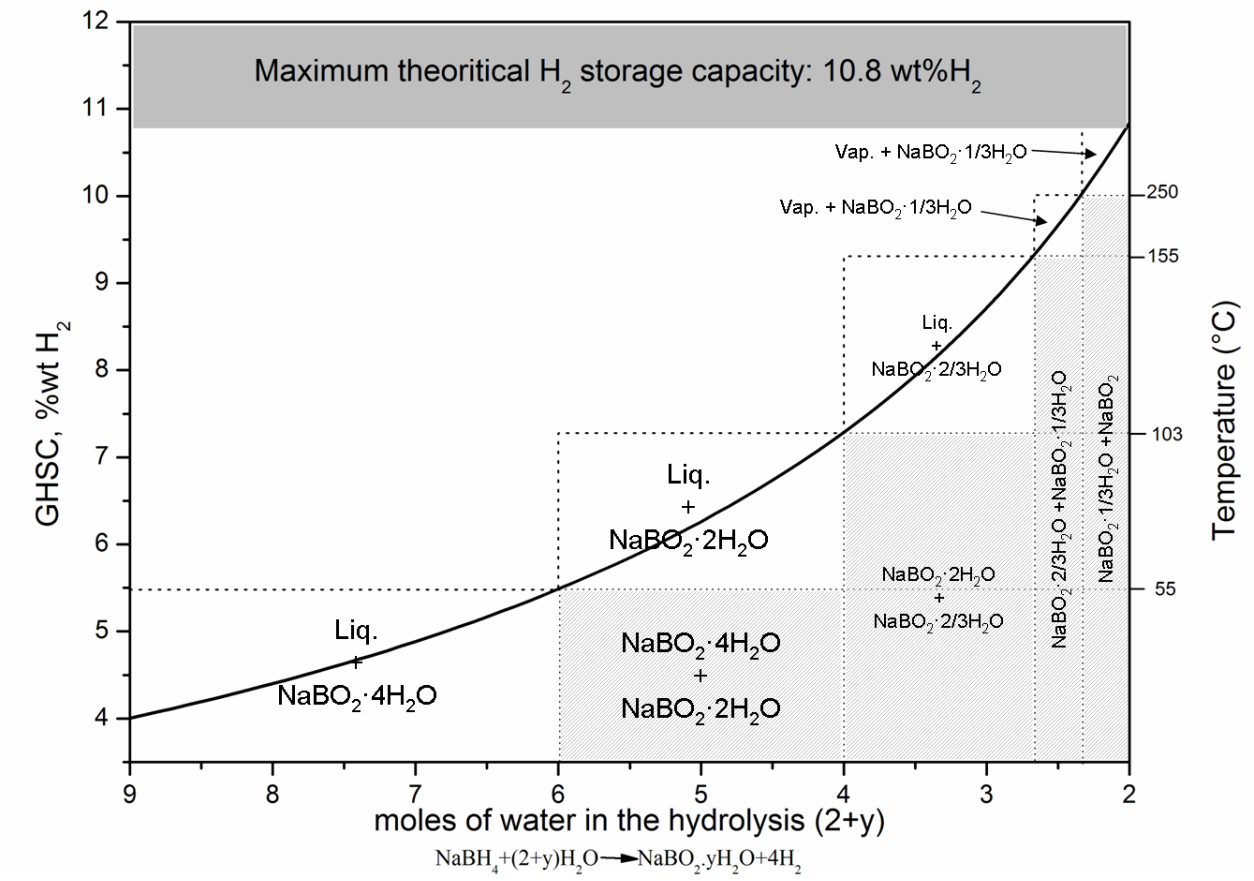

Figure 5. GHSC as a function of the hydrolysis reaction stoichiometry (solid line). Temperature and binary phase domains have been reported (dotted lines and greyed areas) according the revised binary phase diagram.

Scheme 1.

$$NaBH_4(s) + (2+y)H_2O(l) \xrightarrow{cat} NaBO_2 \cdot yH_2O(s) + 4H_2(g) \quad (1)$$

where y = 0,1/2, 1, 2 and 4 [20]

Scheme 2.

$$NaBO_2 \cdot 2/3H_2O + Vap. \xrightarrow{x_{NaBO_2}=0.28;T=131.6°C} Liq. \quad (2)$$

Scheme 3.

$$Ice + NaBO_2 \cdot 4H_2O \xrightarrow{-7\pm2°C} Liq. \quad (3)$$

Scheme 4.

$$NaBO_2 \cdot 2H_2O + Liq. \xrightarrow{55\pm2°C} NaBO_2 \cdot 4H_2O \quad (4)$$

Scheme 5.

$$NaBO_2 \cdot 2/3H_2O + Liq. \xrightarrow{103\pm2°C} NaBO_2 \cdot 2H_2O \quad (5)$$

Scheme 6.

$$NaBO_2 \cdot 1/3H_2O + Vap. \xrightarrow{155\pm2°C} NaBO_2 \cdot 2/3H_2O \quad (6)$$

Scheme 7.

$$NaBO_2 + Vap \xrightarrow{250\pm2°C} NaBO_2 \cdot 1/3H_2O \quad (7)$$

Scheme 8. Relation between x_{NaBO2}, the $NaBO_2$ molar fraction and y, the pseudo hydration degree of borate compounds.

$$x_{NaBO_2} = \frac{1}{1+y} \text{ and } y = \frac{1-x_{NaBO_2}}{x_{NaBO_2}} \quad (8)$$

with $0.2 \leq x_{NaBO_2} \leq 1$ and $0 \leq y \leq 4$

Table 1. Literature data on the stability of borate compounds along the vertical section $NaBO_2$-H_2O of the ternary system Na_2O-B_2O_3-H_2O for different temperatures.

T (°C)	Reported stable borate compounds	Ref.
0	$NaBO_2 \cdot 4H_2O$	[15]
30	$NaBO_2 \cdot 4H_2O$; $NaBO_2 \cdot 2H_2O$	[13]
45	$NaBO_2 \cdot 4H_2O$; $NaBO_2 \cdot 2H_2O$; $NaBO_2 \cdot 1/2H_2O$	[16]
60	$NaBO_2 \cdot 2H_2O$; $NaBO_2 \cdot 1/2H_2O$	[17]
90	$NaBO_2 \cdot 2H_2O$; $NaBO_2 \cdot 1/2H_2O$	[18]
100	$NaBO_2 \cdot 2H_2O$; $NaBO_2 \cdot 1H_2O$, $NaBO_2 \cdot 1/2H_2O$	[19]

Table 2. Identified invariant transformations in the binary phase diagram $NaBO_2$-H_2O.

	Temperature (°C)	Method [a]	Ref.
$NaBO_2 \cdot 2H_2O + Liq. \longrightarrow NaBO_2 \cdot 4H_2O$	56	P-TGA	[20]
	58	P-TGA	[22]
	53	P-Solubility	[26]
$NaBO_2 \cdot 1H_2O + Liq. \longrightarrow NaBO_2 \cdot 2H_2O$	105	P-TGA	[20]
	105	P-Solubility	[26]
	112	P-TGA	[22]
$NaBO_2 \cdot 1/2H_2O + Liq. \longrightarrow NaBO_2 \cdot 1H_2O$	155°C	P-TGA	[20]
	Not observed	P-TGA	[22]
$NaBO_2 + Liq. \longrightarrow NaBO_2 \cdot 1/2H_2O$	260	P-TGA	[20]
	306	P-TGA	[22]

[a] P refers to closed reactor used for the studies, i.e. experiments were supposed to be carried out under pressure for temperature higher than 100 °C.

Table 3. Dehydration step temperatures and related mass losses, after Chiriac et al. [31].

Dehyd. Step	T (°C)	Mass loss (wt.%) [b]
1	46	48.4
2	90	27.2
3	135	23.8
4	162	16.2
5	250	8.4

[b] Mass losses were calculated from $NaBO_2$ final product.

Table 4. Onset temperatures according to DSC experiments.

x_{NaBO2}	Onset temperature (°C)		
	Scheme 3	Scheme 4	Scheme 5
0.021	-7.0	-	-
0.054	-4.7	-	-
0.095	-7.2	-	-
0.161	-7.8	52	-
0.200	-	56.7	-
0.230	-	56.0	-
0.265	-	54.1	-
0.333	-	-	103.5

Table 5. Expected GHSC as a function of the borate compounds formed after $NaBH_4$ hydrolysis.

Compound formed after $NaBH_4$ hydrolysis	Pseudo hydration degree, y	Hydrolysis reaction stoichiometry, (2+y)	GHSC (wt.%)
$NaBO_2 \cdot 4H_2O$	4	6	5.48
$NaBO_2 \cdot 2H_2O$	2	4	7.28
$NaBO_2 \cdot 2/3H_2O$	2/3	8/3	9.31
$NaBO_2 \cdot 1/3H_2O$	1/3	7/3	10.01
$NaBO_2$	0	2	10.83

Appendices

Appendix A

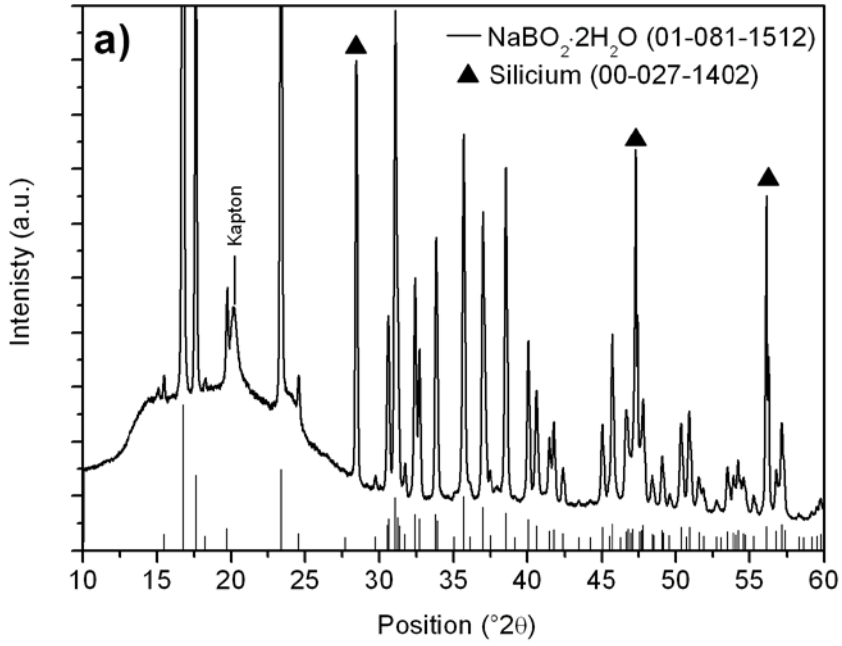

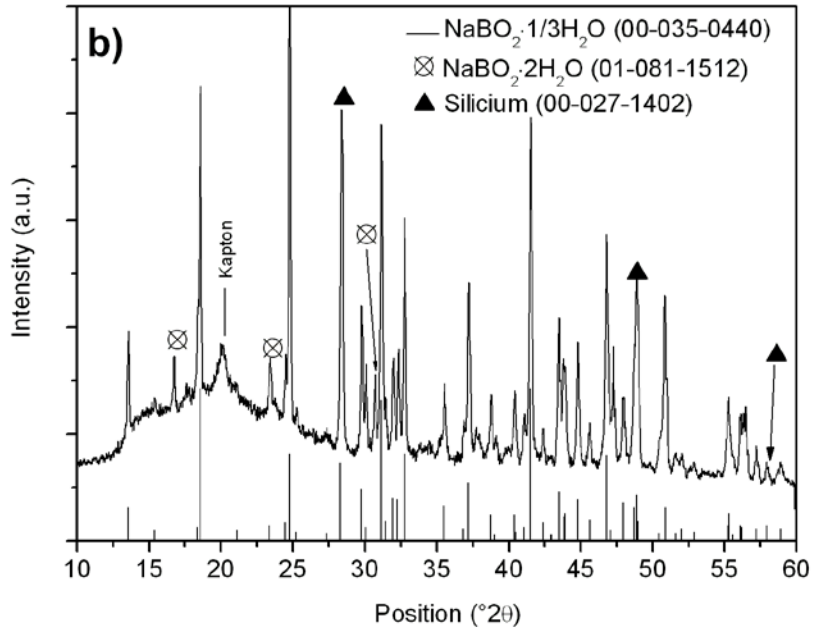

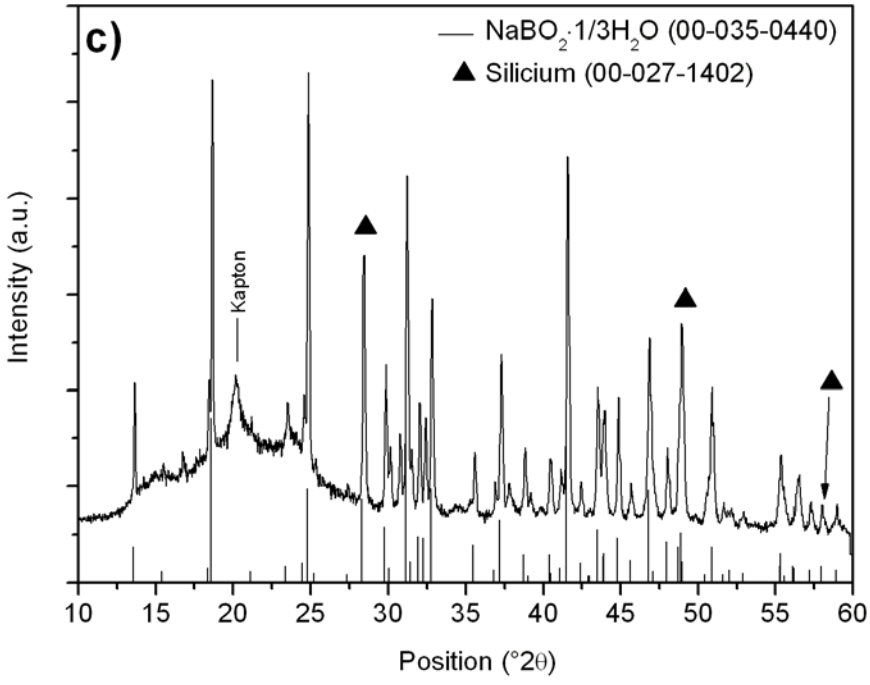
c)
NaBO2·1/3H2O (00-035-0440)
Silicium (00-027-1402)
Kapton
Intensity (a.u.)
Position (°2θ)
10
15
20
25
30
35
40
45
50
55
60

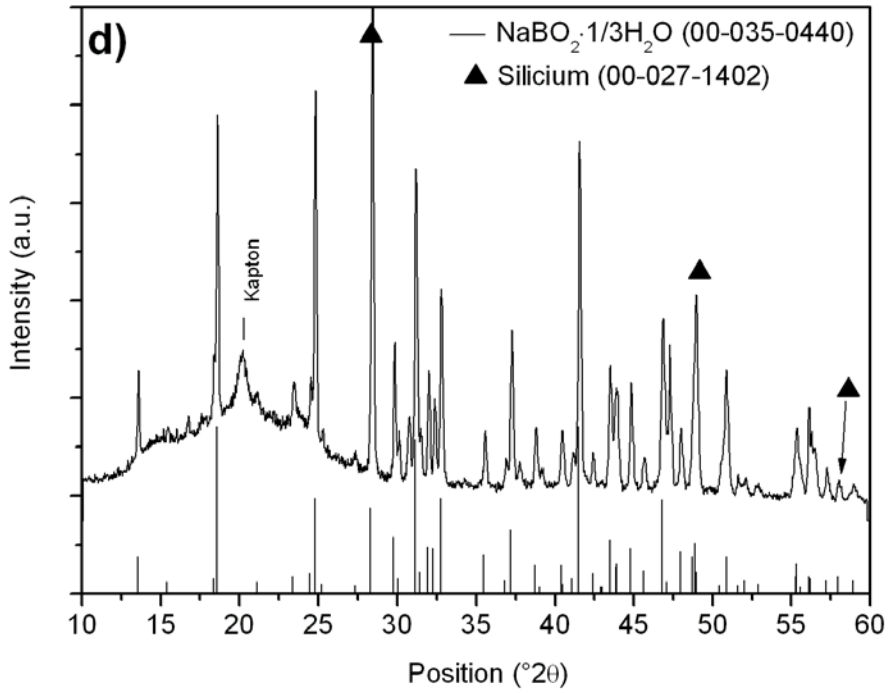
d)
NaBO2·1/3H2O (00-035-0440)
Silicium (00-027-1402)
Kapton
Intensity (a.u.)
Position (°2θ)
10
15
20
25
30
35
40
45
50
55
60

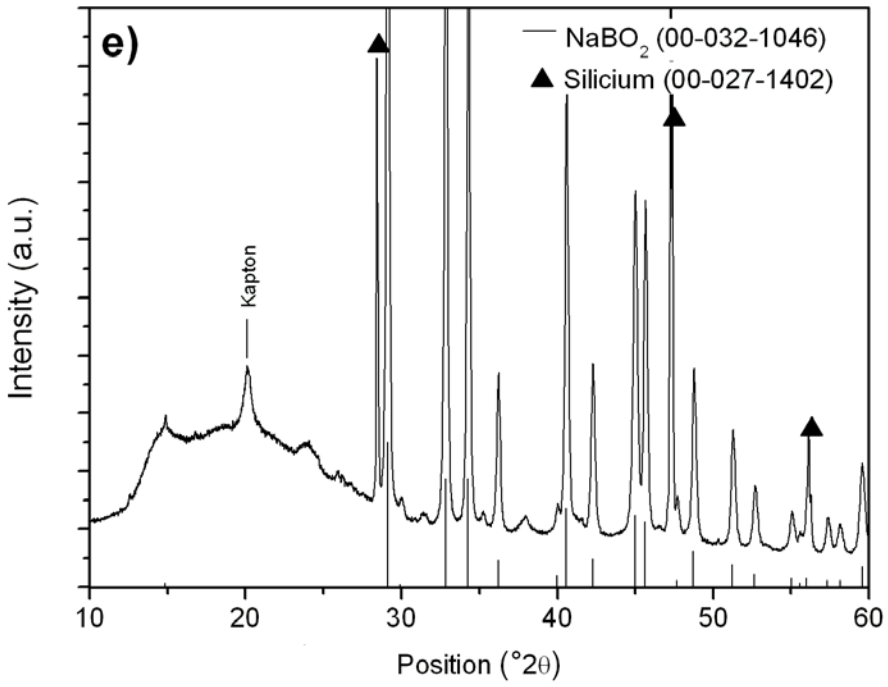

Figure A1. XRD patterns on commercial $NaBO_2 \cdot 4H_2O$ heat treated under inert atmosphere during 3 days at a) 65 °C, b) 110 °C, c) 140 °C, d) 180 °C and e) 300 °C. Comparison with ICDD reference patterns.

Appendix B

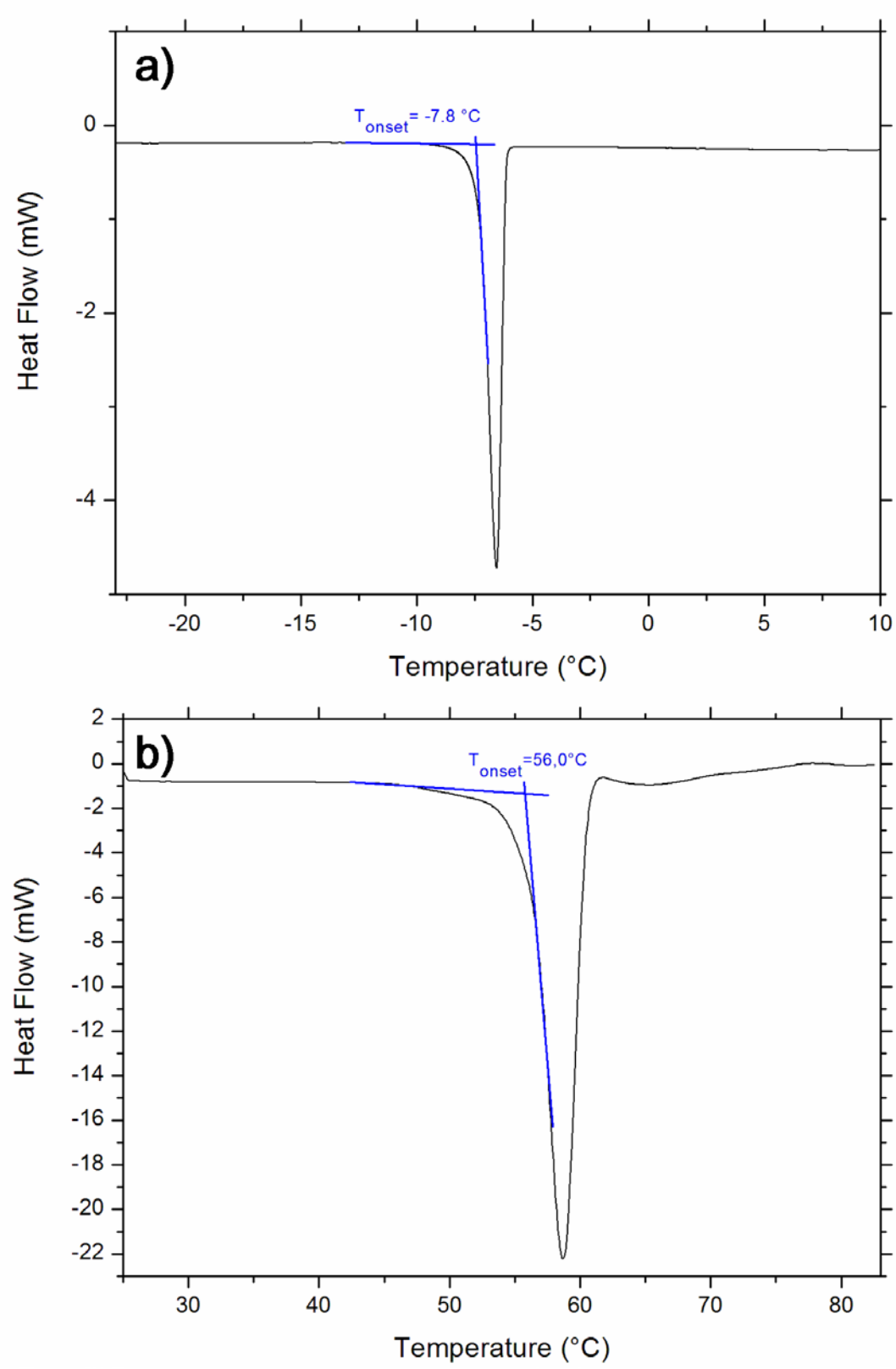
a)
T_{onset} = -7.8 °C
Heat Flow (mW)
0
-2
-4
-20
-15
-10
-5
0
5
10
Temperature (°C)
b)
T_{onset} =56,0°C
Heat Flow (mW)
2
0
-2
-4
-6
-8
-10
-12
-14
-16
-18
-20
-22
30
40
50
60
70
80
Temperature (°C)

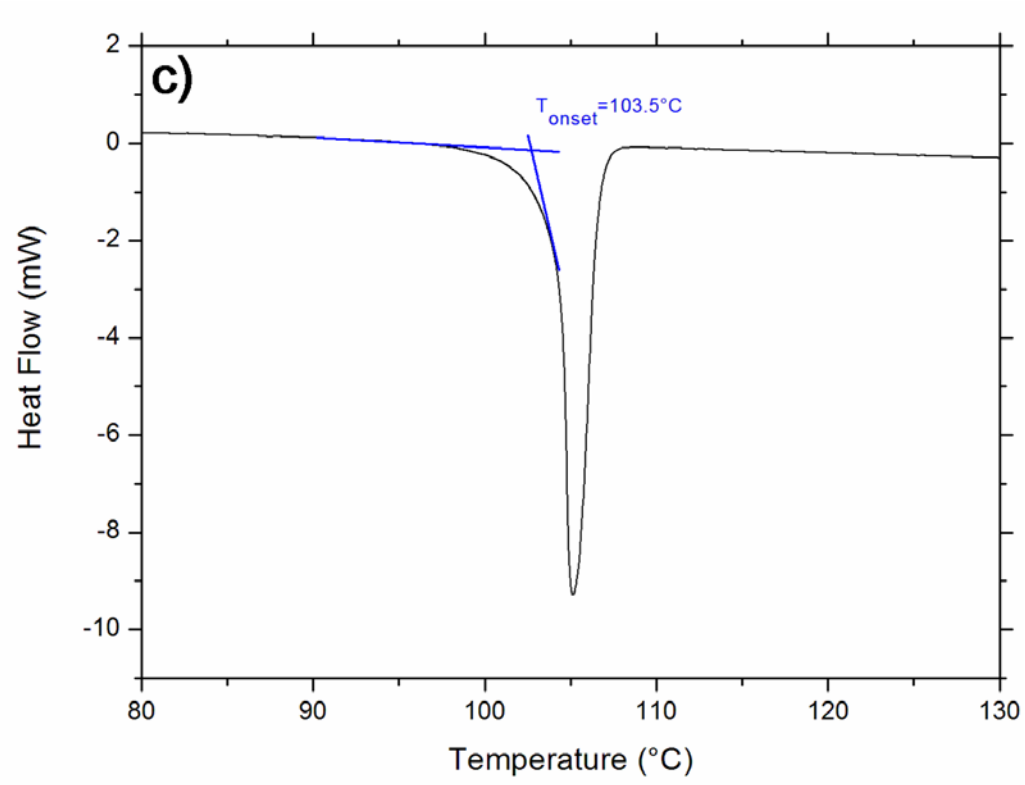

Figure B1. DSC curves for a) x_{NaBO2} = 0.161, b) x_{NaBO2} = 0.230, c) x_{NaBO2} = 0.333.

References

[1] Kojima Y, Suzuki K, Fukumoto K, Sakaki M, Yamamoto T, Kawai Y, et al. Hydrogen generation using sodium borohydride solution and metal catalyst coated on metal oxide. Int J Hydrogen Energy 2002;27:1029–34.

[2] Amendola SC, Sharp-Goldman SL, Janjua MS, Spencer NC, Kelly MT, Petillo PJ, et al. A safe, portable, hydrogen gas generator using aqueous borohydride solution and Ru catalyst. Int J Hydrogen Energy 2000;25:969–75.

[3] Zhao J, Ma H, Chen J. Improved hydrogen generation from alkaline $NaBH_4$ solution using carbon-supported Co-B as catalysts. Int J Hydrogen Energy 2007;32:4711–6.

[4] Andrieux J, Swierczynski D, Laversenne L, Garron A, Bennici S, Goutaudier C, et al. A multifactor study of catalyzed hydrolysis of solid $NaBH_4$ on cobalt nanoparticles: Thermodynamics and kinetics. Int J Hydrogen Energy 2009;34:938–51.

[5] Delmas J, Laversenne L, Rougeaux I, Capron P, Garron A, Bennici S, et al. Improved hydrogen storage capacity through hydrolysis of solid $NaBH_4$ catalyzed with cobalt boride. Int J Hydrogen Energy 2011;36:2145–53.

[6] Damjanovic L, Majchrzak M, Bennici S, Auroux A. Determination of the heat evolved during sodium borohydride hydrolysis catalyzed by Co_3O_4. Int J Hydrogen Energy 2011;36:1991–7.

[7] Prosini PP, Gislon P. Water consumption during solid state sodium borohydride hydrolysis. Int J Hydrogen Energy 2010;35:12234–8.

[8] Liu CH, Kuo YC, Chen BH, Hsueh CL, Hwang KJ, Ku JR, et al. Synthesis of solid-state $NaBH_4$/Co-based catalyst composite for hydrogen storage through a high-energy ball-milling process. Int J Hydrogen Energy 2010;35:4027–40.

[9] Muir SS, Yao, XD. Progress in sodium borohydride as a hydrogen storage material: Development of hydrolysis catalysts and reaction systems. Int J Hydrogen Energy 2011;36:5983–97.

[10] Yang CC, Chen MS, Chen YW. Hydrogen generation by hydrolysis of sodium borohydride

on CoB/SiO_2 catalyst. Int J Hydrogen Energy 2011;36:1418–23.

[11] Marrero-Alfonso EY, Gray JR, Davis TA, Matthews MA. Minimizing water utilization in hydrolysis of sodium borohydride: the role of sodium metaborate hydrates. Int J Hydrogen Energy 2007;32:4723–30.

[12] Laversenne L, Goutaudier C, Chiriac R, Sigala C, Bonnetot B. Hydrogen storage in borohydrides: comparison of hydrolysis conditions of $LiBH_4$, $NaBH_4$ and KBH_4. J Therm Anal Calorim 2008;94:785–90.

[13] Dukelski M. Über borate. Z Anorg Chem 1906;50:38–48. German.

[14] Fang SM. The crystal structure of sodium metaborate. Z Kristallogr Krist 1938;99:1–8.

[15] Rosenheim A, Leyser F. Über polyborate in wässriger lösung. Z Anorg Chem 1921;119:10–20. German.

[16] Sborgi U, Amelotti L. Sui borati Sistema Na_2O-B_2O_3-H_2O a 45°. Gazz Chim Ital 1930;60:468–74. Italian.

[17] Sborgi U, Mecacci F. Sui borati Sistema Na_2O-B_2O_3-H_2O a 60°. Atti Accad Naz Lincei Cl Sci Fis Mat Nat Rend 1916;25:327–32. Italian.

[18] Sborgi U, Sui borati Sistema Na_2O-B_2O_3-H_2O a 90 °. Atti Soc Toscana Sci Nat 1926;35:46–

51. Italian.

[19] Bouaziz R, Milman T, Pascal P. Isotherme 100° du ternaire eau-oxyde de sodium-anhydre borique. C R Acad Sci 1963;257:151–3. French.

[20] Bouaziz R. Borates of lithium and sodium. Ann Chim 1961;6:348-93.

[21] Andrieux J, Goutaudier C, Jeanneau R, Laversenne L, Miele P. Synthesis, characterization and crystal structure of a new trisodium triborate $Na_3[B_3O_4(OH)_4]$. Inorg Chem 2010;49:4830–5.

[22] Toledano P, Benhassaïne A. Sur un appareil d'analyse thermique différentielle sous pression. Etude du système métaborate de sodium-eau. C R Acad Sci 1970;271:1577–80. French.

[23] Block S, Perloff A. The direct determination of the crystal structure of $NaB(OH)_4.2H_2O$. Acta Cryst 1963;16:1233–8.

[24] Csetenyi LJ, Glasser FP, Howie RA. Structure of sodium tetrahydroxyborate. Acta Cryst C 1993;49:1039–41.

[25] Corazza E, Menchetti S, Sabell C. The crystal structure of $Na_3[B_3O_5(OH)_2]$. Acta Cryst B 1975;31:1993–7.

[26] Nies NP, Hulbert RW. Solubility isotherms in the system sodium oxide-boric oxide-water. Revised solubility-temperature curves of boric acid, borax, sodium pentaborate, and sodium

metaborate. J Chem Eng Data 1967;12:303–13.

[27] Blasdale WC, Slansky CM. The solubility curves of boric acid and the borates of sodium. J Am Chem Soc 1939;61:917–20.

[28] Stepanov N, Uvarov V, Popov I, Sasson Y. Study of by-product of $NaBH_4$ hydrolysis and its behaviour at a room temperature. Int J Hydrogen Energy 2008;33:7378–84.

[29] Krzhizhanovskaya MG, Sennova NA, Bubnova RS, Filatov SK. Thermal behaviour of mineral series Borax–Tincalconite–Kernite. Proc Russ Min Soc 1999;121:115–8.

[30] Adams RM. Boron, metallo-boron compounds and boranes. 1st ed. New York : Interscience Publishers; 1964.

[31] Chiriac R, Sigala C, Andrieux J, Laversenne L, Goutaudier C, Miele P. Thermogravimétrie haute résolution (MaxRes) appliquée à l'optimisation des rendements de l'hydrolyse du $NaBH_4$ pour le stockage de l'hydrogène. Spectra Anal 2008;264:41–3. French.

[32] Anderson JL, Eyring EM, Whittaker MP. Temperature jump rate studies of polyborate formation of aqueous boric acid. J Phys Chem 1964;68:1128–32.

[33] Edwards JO, Morrison GC, Ross VF, Schultz JW. The structure of the aqueous borate ion. J Am Chem Soc 1955;77:266–8.

[34] Andrieux J. Stockage de l'hydrogène dans les borohydrures alcalins, hydrolyse du borohydrure de sodium [dissertation]. Lyon(France): Université Lyon1;2010. French.

[35] Jensen EH. A study on sodium borohydrides with special reference to its analytical application in organic chemistry. 1st ed. Copenhagen : Nyt. Nordisk Forlag; 1954.

[36] Schlesinger HI, Brown HC, Finholt AE, Gilbreath JR, Hockstra HR, Hyde EK. Sodium borohydride, its hydrolysis and its use as a reducing agent and in the generation of hydrogen. J Am Chem Soc 1953;75:215–9.

[37] Kaufman CM, Sen B. Hydrogen generation by hydrolysis of sodium tetrahydroborate: effects of acids and transition metals and their salts. J Chem Soc Dalton Trans 1985;2:307–13.

[38] Liu BH, Li ZP, Suda S. Nickel- and cobalt-based catalysts for hydrogen generation by hydrolysis of borohydride. J Alloys Compd 2006;415:288–93.

[39] Gardiner JA, Collat JW. Kinetics of the stepwise hydrolysis of tetrahydroborate ion. J Am Chem Soc 1965;87:1692–700.

[40] Zhang J, Fisher TS, Gore JP, Hazra D, Ramachandran PV. Heat of reaction measurements of sodium borohydrides alcoholysis and hydrolysis. Int J Hydrogen Energy 2006;31:2292–8.

[41] Gislon P, Monteleone G, Prosini PP. Hydrogen production from solid sodium borohydride. Int. J. Hydrogen Energy 2009;34:929–37.

[42] Kim JH, Choi KH, Choi YS. Hydrogen generation from solid $NaBH_4$ with catalytic solution for planar air-breathing proton exchange membrane fuel cells. Int J Hydrogen Energy 2010;35:4015–9.

[43] Liu BH, Li ZP, Suda S. Solid sodium borohydride as a hydrogen source for fuel cells. J Alloys Compd 2009;468:493–8.

[44] Fichtner M, Zhao-Karger Z, Hu JJ, Roth A, Weidler P. The kinetic properties of $Mg(BH_4)_2$ infiltrated in activated carbon. Nanotechnology 2009;20:204029.

[45] Sartori S, Knudsen KD, Zhao-Karger Z, Gil Bardaji E, Muller J, Fichtner M, et al. Nanoconfined magnesium borohydrides for hydrogen storage applications investigated by SANS and SAXS. J Phys Chem C 2010;114:18785–9.